JOURNAL OF AGRICULTURAL AND FOOD CHEMISTRY

Article

pubs.acs.org/JAFC

Probing the Binding of the Flavonoid Diosmetin to Human Serum Albumin by Multispectroscopic Techniques

Guowen Zhang,* Lin Wang, and Junhui Pan

State Key Laboratory of Food Science and Technology, Nanchang University, No. 235, Nanjing East Road, Nanchang 330047, China

ABSTRACT: The binding mechanism of molecular interaction between diosmetin and human serum albumin (HSA) in a pH 7.4 phosphate buffer was studied using atomic force microscopy (AFM) and various spectroscopic techniques including fluorescence, resonance light scattering (RLS), UV−vis absorption, circular dichroism (CD), and Fourier transform infrared (FT−IR) spectroscopy. Fluorescence data revealed that the fluorescence quenching of HSA by diosmetin was a static quenching procedure. The binding constants and number of binding sites were evaluated at different temperatures. The RLS spectra and AFM images showed that the dimension of the individual HSA molecules were larger after interaction with diosmetin. The thermodynamic parameters, ΔH° and ΔS° were calculated to be −24.56 kJ mol^{-1} and 14.67 J mol^{-1} K^{-1}, respectively, suggesting that the binding of diosmtin to HSA was driven mainly by hydrophobic interactions and hydrogen bonds. The displacement studies and denaturation experiments in the presence of urea indicated site I as the main binding site for diosmetin on HSA. The binding distance between diosmetin and HSA was determined to be 3.54 nm based on the Förster theory. Analysis of CD and FT−IR spectra demonstrated that HSA conformation was slightly altered in the presence of diosmetin.

KEYWORDS: *human serum albumin, diosmetin, fluorescence spectroscopy, atomic force microscopy, circular dichroism*

INTRODUCTION

The interaction between macromolecules (e.g., proteins) and drugs has attracted great interest among researchers in recent years.[1−4] Serum albumin, the major transport proteins in the blood circulatory system (accounting for 52−60% of the total plasma protein), functions in the binding and transportation of various ligands such as dyes, fatty acids, and drugs.[5−7] It is known that the distribution, free concentration, and the metabolism of various drugs are strongly affected by drug−protein interactions in the bloodstream. However, drug−protein interactions are known to induce conformational change in a protein.[8] Therefore, the studies of serum albumin−drug interactions have major biochemical importance and should be considered as crucial factors in drug development.

Human serum albumin (HSA) is the most important and abundant constituent of blood plasma, which is a globular protein composed of 585 amino acid residues in a single polypeptide chain cross-linked with 17 disulfide bonds. Nowadays, the domain model of HSA tertiary structure is accepted, according to which the molecule of HSA consists of 3 practically identical domains (I−III), each of them in turn consists of two subdomains (A and B).[9] The internal zone of each domain is composed of hydrophobic amino acid residues, and the external zone of each domain consists of hydrophilic amino acid residues. The domains are placed at angles to each other, and their mutual relationships are described by a model in the shape of a heart.[10] The sole tryptophan residue in HSA is located in Sudlow's site I (Trp-214), which makes it very convenient to study the protein by intrinsic fluorescence.

Diosmetin (3′,5,7-trihydroxy-4′methoxyflavone, structure shown in Figure 1), a flavone, is present in plants belonging to the genus *Teucrium* (Lamiaceae) and in Portuguese olive (*Olea europaea* L.) leaf.[11,12] It exhibits various therapeutic activities, including anti-inflammatory, antivenous thrombosis, and antioxidant/free radical scavenging.[13,14] Recently, Androutsopoulos et al.[15] reported that diosmetin can inhibit proliferation of human breast cancer cells and cause a selective block in the G1 phase of the cell cycle. Because of its biological and pharmacological activities, the study of the binding of diosmetin to HSA is important and will lead to a better understanding of the transport and distribution of flavonoids in blood.

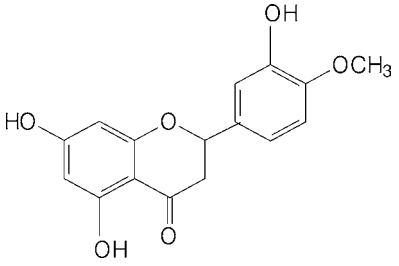

Figure 1. Molecular structure of diosmetin.

Many spectroscopic techniques, such as fluorescence, UV−vis absorption, circular dichroism (CD), and Fourier transform infrared (FT−IR) spectroscopy have become popular methods for revealing protein−drug interactions and structural characterization of proteins because of their high sensitivity, reproducibility, and convenience. They allow noninstrusive measurements of substances in low concentration under physiological conditions.[16] Unfolding studies of protein will

Received: December 21, 2011
Revised: February 21, 2012
Accepted: February 21, 2012
Published: February 21, 2012

provide powerful means for understanding important structural and functional characteristics of the native molecule.

To the best of our knowledge, the interaction between diosmetin and HSA has not been previously reported. The objective of this work was to explore the binding mechanism of diosmetin to HSA and the effect of diosmetin on the conformational changes of the protein in detail by atomic force microscopy and multispectroscopic methods. We hope that this study can provide important insight into the clinical research and the theoretical basis for pharmacology.

MATERIALS AND METHODS

Chemicals and Reagents. Essentially fatty acid free HSA was purchased from Sigma Chemical Company (St. Louis, USA) and used without further purification. The stock solution of HSA (1.0×10^{-4} mol L^{-1}) was prepared with 0.1 mol L^{-1} phosphate buffer of pH 7.4 containing 0.10 mol L^{-1} NaCl and then diluted to the required concentrations with the buffer. Diosmetin (analytical grade) was obtained from National Institute for the Control of Pharmaceutical Biological Products (Beijing, China). The stock solution (3.33×10^{-3} mol L^{-1}) of diosmetin was prepared in ethanol. Although high concentrations of ethanol affect protein structure,[17] the amount used in making the CD and FT−IR spectra measurements was very small (the maximum ethanol concentrations of sample solution in the CD and FT−IR spectra measurements were 2.4% and 1.9%, respectively). All other reagents and solvents were of analytical reagent grade, and aqueous solutions were prepared with ultrapure water from a Millipore Simplicity water purification system (Millipore, Molsheim, France). All stock solutions were stored at 0−4 °C.

Instrumentations. All fluorescence spectra were measured on a Hitachi spectrofluorimeter Model F-4500 (Hitachi, Japan) equipped with a 150 W xenon lamp and a thermostat bath. The widths of both the excitation slit and emission slit were set at 5.0 nm. The absorption spectra were measured on a Shimadzu UV-2450 spectrophotometer (Shimadzu, Japan). A quartz cell of 1.0 cm was used for the measurements. The circular dichroism spectra were recorded on a Bio-Logic MOS 450 CD spectrometer (Bio-Logic, France) using a 1.0 mm path length quartz cuvette. FT−IR spectra were measured on a Thermo Nicolet-5700 FT−IR spectrometer (Thermo Nicolet Co., USA) equipped with a germanium attenuated total reflection (ATR) accessory, a DTGS KBr detector, and a KBr beam splitter. All FT−IR spectra were recorded via the ATR method with a resolution of 4 cm^{-1} and 60 scans. AFM measurements were carried out on a AJ-V atomic force microscope (AJ Nanotechnology development Co., Ltd., Shanghai, China). The samples were imaged in air with AFM. All experiments, unless specified otherwise, were carried out at room temperature.

Fluorescence Measurements. A quantitative analysis of the potential interaction between diosmetin and HSA was performed by fluorimetric titration. A 3.0 mL solution containing 2.0×10^{-6} mol L^{-1} HSA was added to the quartz cuvette, then titrated by successive addition of the 1.67×10^{-3} mol L^{-1} stock solution of diosmetin with a trace syringe (to give a concentration ranging from 0 to 2.95×10^{-5} mol L^{-1}). The fluorescence emission spectra were recorded at three temperatures (298, 304, and 310 K) in the wavelength range of 290−455 nm with excitation wavelength at 280 nm. The scan speed was 2400 nm min^{-1}.

The displacement experiments were carried out using different site markers viz., warfarin, ibuprofen, and digitoxin for sites I, II, and III, respectively, by keeping the concentrations of HSA and the markers constant at 2.0×10^{-6} mol L^{-1}, and then gradually adding diosmetin solution (to give a final concentration of 2.95×10^{-5} mol L^{-1}). Fluorescence quenching spectra were recorded at 298 K in the range of 285−465 nm. The appropriate blank corresponding to the buffer solution was subtracted to correct the background of fluorescence. The binding constants of HSA−diosmetin systems in the presence of the above site markers were calculated by the fluorescence data.

Fluorescence Anisotropy Experiment. The anisotropy (r) is defined as the difference between the fluorescence intensity emitted in parallel and perpendicular (I_{VV} and I_{VH}) divided by the total intensity. The fluorescence anisotropy experiment was accomplished as follows: a 3.0 mL solution, containing 2.0×10^{-6} mol L^{-1} HSA and 2.0×10^{-6} mol L^{-1} diosmetin, was titrated by successive additions of site marker (warfarin, ibuprofen, or digitoxin). The samples were measured on a Hitachi spectrofluorimeter Model F-4500 in a pH 7.4 phosphate buffer solution at room temperature. The widths of both the excitation slit and emission slit were set at 5.0 nm. Fluorescence anisotropy was calculated from fluorescence intensity measurement employing a vertical excitation polarizer and vertical and horizontal emission polarizers according to eq 1:[18]

$$r = (I_{VV} - GI_{VH})/(I_{VV} + 2GI_{VH}) \quad (1)$$

where I_{VV} and I_{VH} are the intensities obtained with the excitation polarizer oriented vertically and the emission polarizer oriented in vertical and horizontal orientations, respectively. G is the instrument grating correction factor; $G = I_{HV}/I_{HH}$; I refers to the parameters similar to those mentioned above for the horizontal position of the excitation polarizer.

Resonance Light Scattering (RLS) and UV−Vis Absorption Spectra. An appropriate aliquot of HSA solutions was added to a fixed volume of diosmetin solution and diluted to 10 mL with the phosphate buffer solution (pH 7.4). RLS spectra were obtained by synchronous scanning on the spectrofluorometer with the wavelength range of 200−700 nm at room temperature. The widths of both the excitation slit and emission slit were set at 5 nm. The UV−vis absorption spectra of diosmetin were recorded over a wavelength range of 285−495 nm in the phosphate buffer solution (pH 7.4) at room temperature.

Atomic Force Microscopy (AFM) Measurements. AFM measurements were carried out at room temperature using a AJ-V atomic force microscope equipped with a 33 μm tripod scanner, in tapping mode, using pyramidal cantilevers (NT-MDT Corporation, Russia) with probes at a scan frequency of 1 Hz. Samples were prepared by deposition of 5 μL of the samples on freshly cleaved mica plates and were dried overnight, and the AFM measurements were then performed.

Preparation of Different Conformers of HSA. HSA exists in different conformational states as native (N), fast moving (F), and urea induced intermediate (I) forms.[19] The N, F, and I conformations were prepared by mixing 200 μL of HSA monomer stock solution (1.0×10^{-4} mol L^{-1}) with 9800 μL of pH 7 (6.0×10^{-2} mol L^{-1} phosphate) and pH 3.5 (1.0×10^{-2} mol L^{-1} acetate) buffers and the desired volumn of urea stock solution (10 mol L^{-1}) prepared in pH 7 phosphate buffer. The existence of different isomers in the experimental preparations was confirmed with various fluorescence properties of different forms. The final solution mixtures (10.0 mL) were incubated for 10−12 h at room temperature before optical measurements.

Circular Dichroism (CD) Studies. The CD spectra of HSA (2.0×10^{-6} mol L^{-1}) in the presence of diosmetin were recorded in the range of 190−250 nm at room temperature under constant nitrogen flush. The molar ratios of diosmetin to HSA were varied as 0:1, 1:1 and 4:1. All observed CD spectra were baseline subtracted for phosphate buffer (pH 7.4), and results were taken as CD ellipticity in mdeg. The contents of secondary conformation forms of HSA, e.g., α-helix, β-sheet, β-turn, and random coil, were analyzed from CD spectroscopic data by the online SELCON3 program. More information about the program is available at the following Web site: http://dichroweb.cryst.bbk.ac.uk/html/home.shtml.

FT−IR Measurements. FT−IR measurements were performed on a Nicolet-5700 FT−IR spectrometer (USA). All spectra were taken via the ATR method with a resolution of 4 cm^{-1} and 60 scans. The FT−IR spectra of HSA (2.0×10^{-6} mol L^{-1}) in the absence and presence of diosmetin were recorded in the range of 1800−1400 cm^{-1} at pH 7.4 phosphate buffer and room temperature. The molar ratio of diosmetin to HSA was maintained at 4:1. The corresponding absorbance contributions of buffer and free diosmetin solutions were recorded and

digitally subtracted at the same condition. The secondary structure compositions of free HSA and its diosmetin complex were estimated by the FT−IR spectra and the curve-fitted results of the amide I band.

RESULTS AND DISCUSSION

Fluorescence Quenching. Fluorescence quenching is the decrease of the quantum yield of fluorescence from a

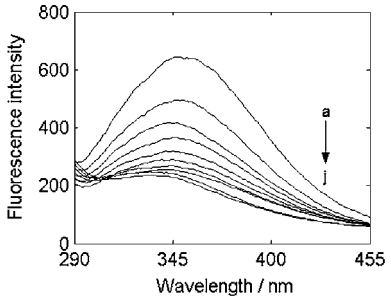

Figure 2. Emission spectra of HSA in the presence of diosmetin at different concentrations (pH 7.4, T = 298 K, λ_{ex} = 280 nm, λ_{em} = 346 nm). c(HSA) = 2.0 × 10^{-6} mol L^{-1}, and c(diosmetin) = 0, 0.33, 0.67, 1.00, 1.33, 1.65, 1.98, 2.31, 2.63, and 2.95 × 10^{-5} mol L^{-1} for curves a−j, respectively.

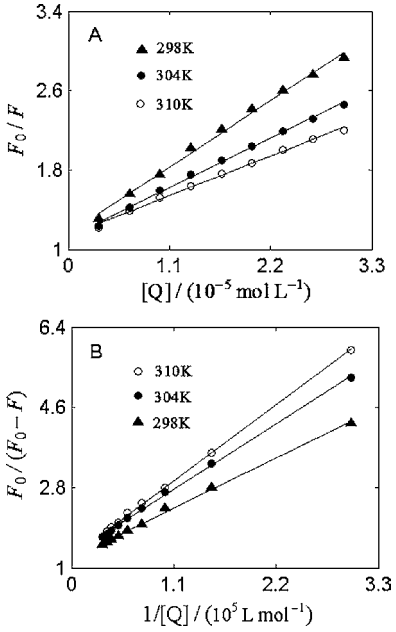

Figure 3. The Stern−Volmer plots (A) and modified Stern−Volmer plots (B) for the HSA−diosmetin system at three different temperatures.

fluorophore induced by a variety of molecular interactions, such as excited-state reactions, molecular rearrangements, ground-state complex formation, collisional quenching, and

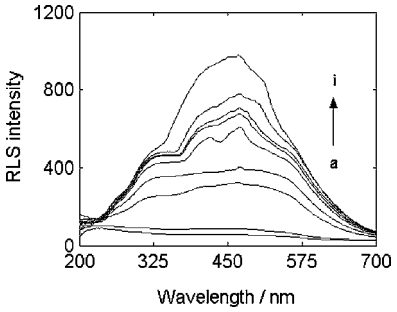

Figure 4. RLS spectra of the HSA−diosmetin system at pH 7.4 and room temperature. Curves: (a) c(diosmetin) = 0 and c(HSA) = 2.0 × 10^{-6} mol L^{-1}; (b) c(diosmetin) = 2.0 × 10^{-6} mol L^{-1}, c(HSA) = 0; c(HSA) = 0.2, 0.4, 0.6, 0.8, 1.0, 1.2, and 1.4 × 10^{-6} mol L^{-1} for curves c−i, respectively, and c(diosmetin) = 2.0 × 10^{-6} mol L^{-1}.

energy transfer.[20] The different mechanisms of quenching are usually classified as either dynamic quenching or static quenching. Dynamic and static quenchings can be distinguished by their different dependence on temperature and viscosity, or preferably by lifetime measurements. For dynamic quenching, higher temperatures result in faster diffusion and larger amounts of collisional quenching. The quenching constant increases with increasing temperature, but the reverse effect would be observed for static quenching.[21] The fluorescence spectra of HSA in the presence of diosmetin at different concentrations are shown in Figure 2. It can be observed in Figure 2 that HSA exhibited a strong fluorescence emission peak at 346 nm after being excited with a wavelength of 280 nm. With the addition of diosmetin, the fluorescence intensity of HSA showed significant decrease with an obvious shift of the peak toward shorter wavelength (from 346 to 332 nm), which indicated that diosmetin could interact with HSA and quench its intrinsic fluorescence, and the microenvironment of tryptophan residue in HSA was changed, leading to an increase of hydrophobicity in the vicinity of this residue.[22]

To elaborate the fluorescence quenching mechanism, the well-known Stern−Volmer equation was utilized for the data analysis:

$$\frac{F_0}{F} = 1 + K_{SV}[Q] = 1 + K_q\tau_0[Q] \quad (2)$$

where F_0 and F are the fluorescence intensities of HSA in the absence and presence of the quencher, respectively. K_{SV}, K_q, τ_0, and [Q] are the Stern−Volmer dynamic quenching constant, the quenching rate constant of the biomolecule ($K_q = K_{SV}/\tau_0$), the average lifetime of the fluorophore in the absence of quencher ($\tau_0 = 10^{-8}$ s[23]), and the concentration of quencher, respectively.

The curves of F_0/F versus [Q] at three different temperatures (298, 304, and 310 K) are displayed in Figure 3A. The corresponding K_{SV} values for the interaction between diosmetin

Table 1. Modified Stern−Volmer Association Constants K_a and Relative Thermodynamic Parameters of the HSA−Diosmetin System

T (K)	K_a (× 10^5 L mol^{-1})	R^a	$\Delta H°$ (kJ mol^{-1})	$\Delta G°$ (kJ mol^{-1})	$\Delta S°$ (J mol^{-1} K^{-1})	R^b
298	1.18 ± 0.02	0.9968	−24.56 ± 0.01	−28.93 ± 0.02	14.67 ± 0.04	0.9999
304	0.97 ± 0.02	0.9994		−29.02 ± 0.02		
310	0.80 ± 0.01	0.9997		−29.11 ± 0.02		

[a] R is the correlation coefficient for the K_a values. [b] R is the correlation coefficient the van't Hoff plot.

dx.doi.org/10.1021/jf205260g | J. Agric. Food Chem. 2012, 60, 2721−2729

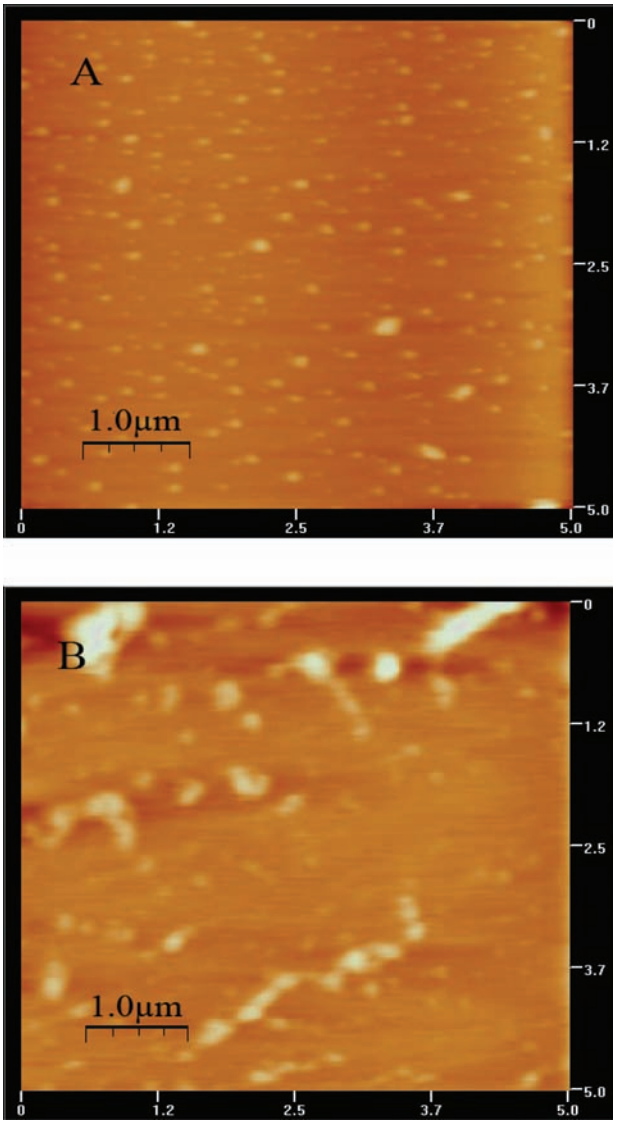

Figure 5. AFM topography images of HSA (A) and the HSA–diosmetin complex (B) adsorbed onto mica with tapping mode in air, and the scan size of the image is 5 μm × 5 μm. c(HSA) = 4.0 × 10^{-9} mol L^{-1}; c(diosmetin) = 2.0 × 10^{-8} mol L^{-1}.

Table 2. Apparent Binding Constant K_b and the Number of Binding Sites n of the HSA–Diosmetin System

T (K)	K_b (× 10^5 L mol^{-1})	n	R^a
298	1.27 ± 0.04	0.84 ± 0.01	0.9995
304	1.10 ± 0.02	0.83 ± 0.04	0.9999
310	0.81 ± 0.06	0.86 ± 0.01	0.9992

[a] R is the correlation coefficient for the K_b values.

and HSA were obtained to be (6.10 ± 0.02) × 10^4 L mol^{-1} (298K, R = 0.9976), (4.53 ± 0.01) × 10^4 L mol^{-1} (304 K, R = 0.9986), and (3.66 ± 0.01) × 10^4 L mol^{-1} (310 K, R = 0.9980), respectively. The values of K_q at different temperatures were calculated to be (6.10 ± 0.02) × 10^{12} L mol^{-1} s^{-1} (298 K), (4.53 ± 0.01) × 10^{12} L mol^{-1} s^{-1} (304 K), and (3.66 ± 0.01) × 10^{12} L mol^{-1} s^{-1} (310 K), respectively. The perfect linear correlation coefficients suggested that the quenching of HSA by diosmetin could be interpreted by the Stern–Volmer equation. The results showed that the K_{SV} values decreased with

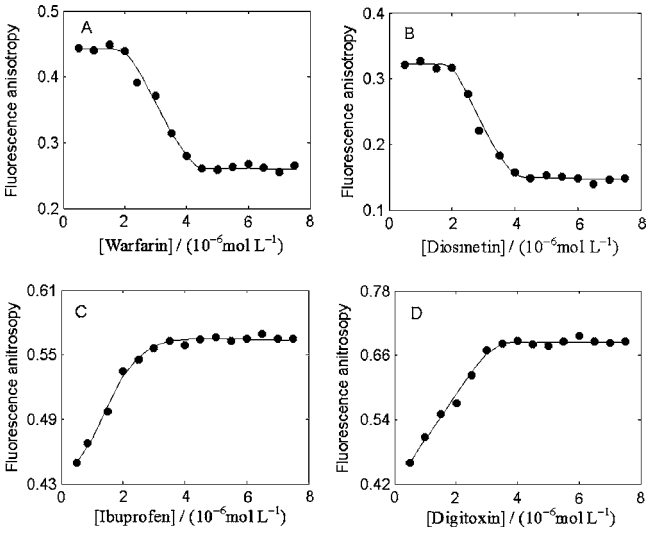

Figure 6. Fluorescence anisotropy values of the HSA–diosmetin complex with different aliquots of warfarin added (A); fluorescence anisotropy values of the warfarin–HSA complex with different aliquots of diosmetin added (B); fluorescence anisotropy values of the HSA–diosmetin complex with different aliquots of ibuprofen (C) or digitoxin (D) added. c(HSA) = 2.0 × 10^{-6} mol L^{-1}.

Table 3. Binding Parameters of Different States of HSA with Diosmetin

HSA isomers	K_a (× 10^5 L mol^{-1})	n
native (N)	1.19 ± 0.02	0.84 ± 0.01
fast moving (F)	0.64 ± 0.06	0.81 ± 0.02
urea induced intermediate (I)	0.56 ± 0.03	0.82 ± 0.01

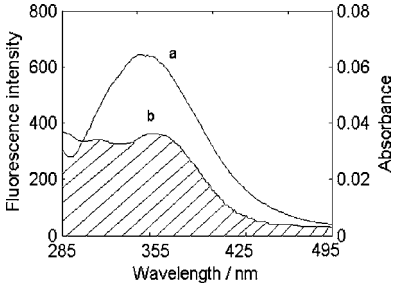

Figure 7. Spectral overlaps of the fluorescence spectra of HSA (a) with the absorption spectra of diosmetin (b). c(HSA) = c(diosmetin) = 2.0 × 10^{-6} mol L^{-1}.

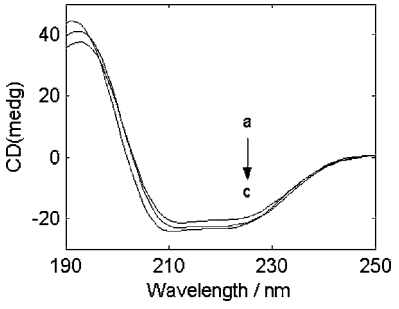

Figure 8. CD spectra of the HSA–diosmetin system in the presence of increasing amounts of diosmetin at pH 7.4 and room temperature. c(HSA) = 2.0 × 10^{-6} mol L^{-1}; the molar ratios of diosmetin to HSA were 0:1 (a), 1:1 (b), and 4:1(c).

dx.doi.org/10.1021/jf205260g | J. Agric. Food Chem. 2012, 60, 2721–2729

Table 4. Secondary Structure of HSA and HSA−Diosmetin Systems (CD Spectra) at pH 7.4

molar ratio [diosmetin]/[HSA]	α-helix (%)	β-sheet (%)	β-turn (%)	random coil (%)
0:1	52.6 ± 1.8	13.5 ± 0.7	14.1 ± 0.8	19.8 ± 1.3
1:1	56.2 ± 1.6	13.9 ± 0.8	12.0 ± 0.9	17.9 ± 0.9
4:1	57.1 ± 2.0	14.8 ± 1.1	11.7 ± 0.6	16.4 ± 1.0

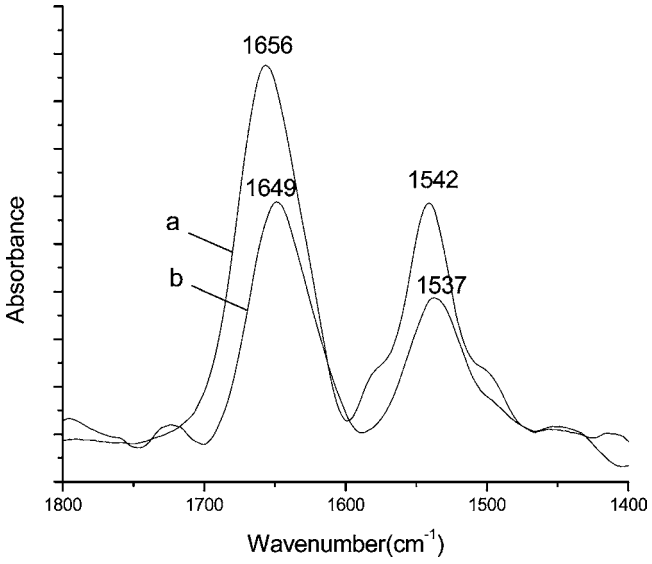

Figure 9. FT−IR spectra of free HSA (a) and difference spectra [(HSA−diosmetin) − diosmetin] (b) at pH 7.4 phosphate buffer in the region of 1800−1400 cm^{-1}; c(HSA) = 2.0 × 10^{-6} mol L^{-1}; the molar ratio of diosmetin to HSA was 4:1.

increasing temperature, and the values of K_q were much greater than the limiting diffusion rate constant of the biomolecule (2 × 10^{10} L mol^{-1} s^{-1}),[24] which suggested that the quenching mechanism of HSA by diosmetin is not initiated by dynamic quenching but by static quenching.[25]

The fluorescence data was further examined by using modified Stern−Volmer equation:[26]

$$\frac{F_0}{F_0 - F} = \frac{1}{f_a K_a}\frac{1}{[Q]} + \frac{1}{f_a} \quad (3)$$

where K_a is the modified Stern−Volmer association constant for the accessible fluorophores, and f_a is the fraction of accessible fluorescence. Herein, the modified Stern−Volmer equation was applied to determine K_a by a linear regression of $F_0/(F_0 - F)$ versus $1/[Q]$ (Figure 3B), and the result is listed in Table 1. As shown in Table 1, the decreasing trend of K_a with increasing temperature was in accord with K_{SV}'s dependence on temperature as discussed above, which further confirmed that the fluorescence quenching of HSA is static quenching.

Thermodynamic Analysis. The interaction forces between small molecules and biomolecules mainly include hydrogen bonds, van der Waals forces, electrostatic forces, and hydrophobic interactions. Thermodynamic parameters, e.g., enthalpy change ($\Delta H°$) and entropy change ($\Delta S°$) binding interaction, are the main evidence for confirming the binding force. If there is no significant change in temperature, $\Delta H°$ can be regarded as

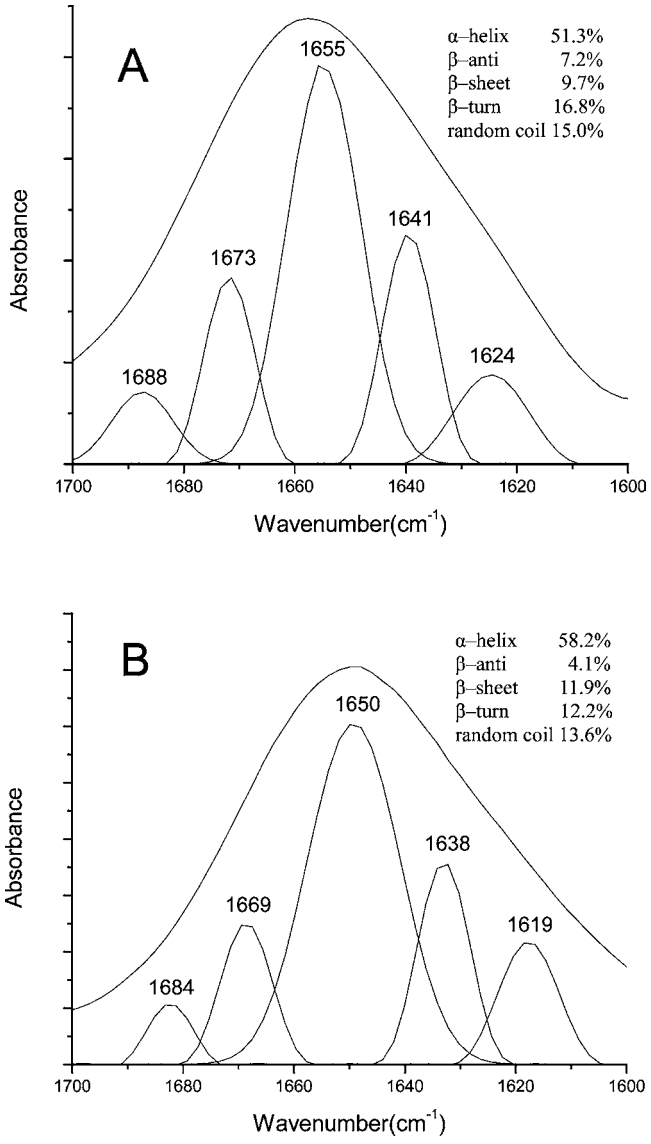

Figure 10. Curve-fitted amide I region (1700−1600 cm^{-1}) of free HSA (A) and its diosmetin complex (B). c(HSA) = 2.0 × 10^{-6} mol L^{-1}; the molar ratio of diosmetin to HSA was 4:1.

a constant, and then the values of $\Delta H°$ and $\Delta S°$ can be estimated from the van't Hoff equation as follows:

$$\log K_a = -\frac{\Delta H°}{2.303RT} + \frac{\Delta S°}{2.303R} \quad (4)$$

where R is the gas constant. The temperatures used were 298, 304, and 310 K. The values of $\Delta H°$ and $\Delta S°$ were obtained from the slope and intercept of the linear van't Hoff plot based on log K_a versus $1/T$ and presented in Table 1. The free energy change ($\Delta G°$) could be calculated from the following equation:

$$\Delta G° = \Delta H° - T\Delta S° \quad (5)$$

As seen from Table 1, the values for $\Delta H°$ and $\Delta S°$ of the binding reaction between diosmetin and HSA were −24.56 kJ mol^{-1} and 14.67 J mol^{-1} K^{-1}, respectively. The positive $\Delta S°$ value is frequently regarded as evidence for a hydrophobic interaction.[27] The negative value of $\Delta H°$ suggested that the binding process is predominately enthalpy driven and by means of hydrogen binding interactions.[28] Therefore, both hydrophobic interactions and hydrogen bonds played a major role in

dx.doi.org/10.1021/jf205260g | J. Agric. Food Chem. 2012, 60, 2721−2729

the binding of diosmetin to HSA and contributed to the stability of the complex.

RLS and AFM Analysis of the HSA−Diosmetin Complex. RLS is a highly sensitive method for the study of aggregation of chromophores on biological macromolecules. RLS spectra of the HSA−diosmetin system in phosphate buffer solution (pH 7.4) are shown in Figure 4. As shown from Figure 4, both free HSA and free diosmetin exhibited very weak RLS signals, but when a fixed concentration of diosmetin was titrated with different amounts of HSA, the intensity of RLS were remarkably enhanced. On the basis of the theory of resonance light scattering,[29] it can be deduced that RLS intensity is related to the size of the formed particle and directly proportional to the square of molecular volume, and Liu et al.[30] have demonstrated that larger particles would induce stronger light scattering signals. Hence, the added HSA likely interacted with diosmetin in solution, and a HSA−diosmetin complex formed, resulting in an increase in the RLS signal.

AFM has been proved to be a very reliable tool for biological applications and for the investigation of protein structure and protein behavior.[31,32] During the experiments, the concentrations of HSA and diosmetin solution were 4.0×10^{-9} and 2.0×10^{-8} mol L^{-1}, respectively, and the pH value was kept at 7.4. The size and surface morphology of HSA and its diosmetin mixture were analyzed by AFM (Figure 5). From Figure 5A, the topography image for HSA molecules adsorbed onto mica can be clearly observed. After averaging the width of 50 single HSA molecules adsorbed onto mica, the mean width and height of the individual HSA molecules were obtained to be 25 ± 4.5 nm and 4.1 ± 2.6 nm, respectively. The measured dimension of HSA was close to that of the molecule in its crystal state.[33] Upon interaction with diosmetin, the HSA molecule appeared to be more swollen on the mica substrate in Figure 5B, and the flocculation observed or aggregation of HSA molecular on the mica substrate can be observed. The mean width and height of the molecules were changed to be 102 ± 9.1 nm and 12.5 ± 3.0 nm, respectively, obviously more than that of the HSA practice size, which could be a result of the interaction between HSA and diosmetin. Protein−protein hydrophobic interaction is also an important factor that leads to protein aggregation.[34] After interaction with diosmetin, the microenvironment around the HSA molecule was changed and the protein molecule exposed to a more hydrophobic environment. In order to minimize the number of unfavorable factors to form a stable structure, the HSA molecule reduced the surface area in contact with water by molecular aggregation. Therefore, we can see bigger molecules on the mica substrate, and this result also revealed that there were hydrophobic interactions between HSA and diosmetin. The AFM result confirmed the deduction from RLS experiment.

Identification of the Binding Sites of Diosmetin on HSA. When small molecules bind independently to a set of equivalent sites on a macromolecule, the apparent binding constant (K_b) and the number of binding sites (n) can be obtained from the double logarithm regression curve of log $[(F_0 - F)/F]$ versus log [Q] according to the following equation:

$$\log \frac{F_0 - F}{F} = \log K_b + n \log[Q] \quad (6)$$

From eq 6, the values of K_b and n of the HSA−diosmetin system are summarized in Table 2. The calculated K_b values suggested that a moderate affinity existed between HSA and diosmetin, and the values of K_b decreased with the increasing temperature indicating that the capacity of diosmetin binding to HSA was reduced. The increasing temperature results in the increasing diffusion coefficient and the reduction of stability of the HSA−diosmetin complex. The high linear correlation coefficient ($R > 0.998$) at different temperatures indicated the assumptions underlying the derivation of eq 6 were valid. The values of n are approximately equal to 1 suggesting that there was a single class of binding sites on HSA for diosmetin.

In order to identify the drug binding site on HSA, displacement binding experiments have been commonly carried out using some probes that specifically bind to a known site or region on HSA. Sudlow et al.[35] have suggested two main distinct binding sites on HSA, sites I and II, which locate in the hydrophobic cavities of subdomains IIA and IIIA, respectively. Sites I and II of protein show affinity for warfarin and ibuprofen, respectively. The binding of digitoxin was found to be independent of sites I and II,[36] which was defined as site III. In the present study, warfarin, ibuprofen, and digitoxin were selected as site markers to identify the diosmetin binding site on HSA. Various amounts of diosmetin were added to a solution containing fixed concentrations of HSA and site markers, and then the fluorescence emission spectra were measured with the excitation wavelength at 280 nm. The fluorescence data were analyzed by the modified Stern−Volmer equation. The corresponding association constants of HSA−diosmetin in the presence of warfarin, ibuprofen, and digitoxin were calculated to be $(0.41 \pm 0.04) \times 10^5$, $(1.09 \pm 0.02) \times 10^5$, and $(1.02 \pm 0.01) \times 10^5$ L mol^{-1} at 298 K, respectively. Compared with the association constant ($1.18 \pm 0.02 \times 10^5$ L mol^{-1}) of the HSA−diosmetin system in the absence of the site markers, it was obvious that the value of the association constant decreased remarkably with the addition of warfarin, whereas it remained almost the same with the addition of ibuprofen or digitoxin. The results suggested that the binding site for diosmetin and warfarin was same on HSA, that is to say, diosmetin was most likely located in region of subdomain IIA (Sudlow site I).

Further evidence regarding the binding site of diosmetin on HSA was obtained by fluorescence anisotropy tests. The fluorescence anisotropy can give information about the rotational rate of the solute molecule.[37] Now we come to the fluorescence anisotropy of diosmetin competitive with the site marker (warfarin, ibuprofen, or digitoxin) on the binding region of HSA. As shown in Figure 6A, the fluorescence anisotropy was unchanged with warfarin added to the HSA−diosmetin system in a concentration ranging from 0 to 2.0×10^{-6} mol L^{-1} and thereafter decreased remarkably, which could be explained by the affinity of ligand binding to HSA.[38] The turning point of the anisotropy was approximately the equimolar of the ternary mixture, suggesting that diosmetin was displaced by warfarin upon addition of warfarin.[39] To further validate the result, we considered diosmetin as a probe, and the diosmetin solution was titrated into the HSA−warfarin system. It can be observed from Figure 6B that with increasing the amounts of diosmetin, the change in anisotropy of the HSA−warfarin system displayed similarly to the behavior of the HSA−diosmetin complex, which indicated that diosmetin shared a common binding site with warfarin. In contrast, the anisotropy of the HSA−diosmetin complex increased gradually upon increasing the concentration of ibuprofen or digitoxin (from 0 to 4.0×10^{-6} mol L^{-1}) (Figure 6C and D), and then the anisotropy was constant, which might be attributed to the fact that more and more ibuprofen or digitoxin molecules bound to the HSA−

diosmetin complex, resulting in its rotational motion being restricted.[18,23] From the above experimental results, it can be concluded that diosmetin was mainly located in the region of site I on HSA.

Denaturation Experiments. The protein unfolding pathway induced by acid and urea was employed to locate the binding site for diosmetin on HSA. HSA undergos N−F and N−I transitions induced by the acidic pH between 7.0 and 3.5 and the urea concentration in the range of 4.8−5.2 mol L^{-1}, respectively.[40] At pH 3.5, the F isomer is dominant, which is characterized by unfolding and separation of domain III, without significantly affecting the rest of the molecule, and isomer I is characterized by the unfolding of domain III and partial but significant loss of the native conformation of domain I. Domain II is known to be unaffected by either N−F or N−I transitions.[19] As seen in Table 3, the number of binding sites of these conformational states were almost similar to that of native HSA (∼1), and this indicated that the binding site for diosmetin is maybe located in domain II of HSA. The decreased binding constant can be understood to be the result of the loss of complex inter- and intradomain interactions that stabilize the albumin structure. A domain in the presence of other unfolded domains cannot be expected to fully reflect its behavior compared to native protein as they are connected through various inter domain forces such as salt bridges, hydrophobic interactions, hydrogen bonding, and natural boundaries between domains.[41]

Energy Transfer from HSA to Diosmetin. Fluorescence resonance energy transfer is a distance dependent interaction in which excitation energy is transferred nonradiatively from the donor molecule to the acceptor molecule. According to Föster's theory,[42] the energy transfer efficiency, E, is not only related to the distance between the donor (protein) and acceptor (diosmetin) but also influenced by the critical energy transfer distance R_0, which is as follows:

$$E = 1 - \frac{F}{F_0} = \frac{R_0^6}{R_0^6 + r^6} \tag{7}$$

where r is the distance between the donor and the acceptor, and R_0 is the critical distance, at which the efficiency of transfer is 50%.

$$R_0^6 = 8.79 \times 10^{-25} \kappa^2 N^{-4} \Phi J \tag{8}$$

In eq 8 κ^2 is the orientation factor related to the geometry of the donor and acceptor of dipoles, and $\kappa^2 = 2/3$ is for random orientation as in fluid solution; N is the refractive index of the medium; Φ is the fluorescence quantum yield of the donor in the absence of the acceptor; J is the overlap integral between the fluorescence emission spectrum of the donor and the absorption spectrum of the acceptor (Figure 7), which can be calculated by the following equation:

$$J = \frac{\int_0^\infty F(\lambda)\varepsilon(\lambda)\lambda^4 d\lambda}{\int_0^\infty F(\lambda) d\lambda} \tag{9}$$

where $F(\lambda)$ is the corrected fluorescence intensity of the donor in wavelength range from λ to $\lambda + \Delta\lambda$, and ε (λ) is the extinction coefficient of the acceptor at wavelength λ. For the ligand−HSA interaction, N = 1.336, and Φ = 0.118.[43] According to eqs 7−9, the values of the parameters were obtained to be J = 2.228 cm^3 L mol^{-1}, R_0 = 2.80 nm, E = 0.197, and r = 3.54 nm. As the donor−to−acceptor distance for the HSA−diosmetin system is less than 8 nm and $0.5R_0 < r < 1.5R_0$, this implies that the energy transfer from HSA to diosmetin occurred with high probability.[44]

Analysis of HSA Conformation after Diosmetin Binding. Circular dichroism (CD) is a sensitive technique to monitor the conformational changes in the protein. The CD spectra of HSA in the absence and presence of diosmetin are shown in Figure 8. The CD spectra of HSA showed two negative bands in the UV region at around 208 and 222 nm, which are characteristic of the α-helix of protein, and both contributed to n-π^* transfer for the peptide bond of the α-helical structure.[45] As seen from Figure 8, the CD intensity of HSA increased without any significant shift of the peaks with increasing the molar ratio of diosmetin to HSA (from 0:1 to 4:1), which indicated partial changes in the protein secondary structure with the increase in α-helical content. The contents of different secondary structures of HSA were calculated by the online Dichroweb software and summarized in Table 4. Our results showed that free HSA contained major contents of 52.6% α-helix, 13.5% β-sheet,14.1% β-turn, and 19.8% random coil. Upon diosmetin interaction, there was a definite increase in α−helix from 52.6% to 57.1% and a minor increase in β-sheet from 13.5% to 14.8% with the decrease in random coil and β-turn from 19.8% to 16.4%, and from 14.1% to 11.7%, respectively, at a molar ratio of diosmetin to HSA of 4:1. The increase of protein α-helix structure upon drug interaction was also reported for syringin−HSA adducts.[46]

To confirm the CD results, the conformational changes of HSA after binding with diosmetin were evaluated by FT−IR spectroscopy. IR spectra of proteins exhibit a number of amide bands, which represent different vibrations of the peptide moiety. Among the amide bands of the protein, the amide I band (1700−1600 cm^{-1}, mainly C═O stretch) and amide II band (1600−1500 cm^{-1}, C−N stretch coupled with N−H bending mode) both have a relationship with the secondary structure of protein, and the amide I band is more sensitive to the change of protein secondary structure than the amide II band.[47] The FT−IR spectra of free HSA and the difference spectra after binding with diosmetin (Figure 9) in phosphate buffer solution were recorded. It can be seen that the peak position of the amide I band was shifted from 1656 to 1649 cm^{-1}, while that of amide II band was moved from 1542 to 1537 cm^{-1} together with the changes in the peak shape and peak intensity upon the addition of diosmetin to HSA. These results indicated that diosmetin interacted with both the C═O and C−N groups in the protein polypeptides and resulted in the rearrangement of the polypeptide carbonyl hydrogen-bonding network.[48]

Figure 10 exhibited the curve-fitted spectra of HSA infrared amide I bands before and after the interaction with diosmetin. The component bands of the infrared amide I band were attributed as follows: 1615−1637 cm^{-1} to β-sheet, 1638−1648 cm^{-1} to random coil, 1649−1660 cm^{-1} to α-helix, 1660−1680 cm^{-1} to β-turn, and 1680−1692 cm^{-1} to β-antiparallel structures, respectively.[49,50] On the basis of the curve-fitted results, the percentage of each secondary structure of HSA in the absence and presence of diosmetin was estimated. Compared with the free HSA, it was evident that the contents of α-helix and β-sheet were increased from 51.3% to 58.2% and from 9.7% to 11.9%, while the contents of β-turn, β-antiparallel, and random coil were decreased from 16.8% to 12.2%, from 7.2% to 4.1%, and from 15.0% to 13.6%, respectively, when the

molar ratio of diosmetin to HSA was 4:1. This result was in accord with that obtained above by CD spectroscopy, which demonstrated that the binding of diosmetin to HSA caused the minimal conformational changes in the protein. However, the minimal conformational changes induced the protein to be exposed to a more hydrophobic environment. In order to form a stable sturcture, HSA molecular aggregation took place.

In summary, the binding properties of diosmetin with HSA were investigated by a fluorescence method combined with UV−vis absorption, RLS, CD, FT−IR spectroscopy, and AFM techniques under physiological conditions. The fluorescence quenching of HSA by diosmetin could be attributed to a static quenching mechanism. The calculated thermodynamic parameters suggested that both hydrophobic interactions and hydrogen bonds dominated in the interaction process. The values of *n* revealed the presence of a single class of binding site on HSA. The displacement experiments indicated that the binding of diosmetin to HSA was most likely located within a hydrophobic cavity of subdomain IIA (site I). The value of the binding distance *r* indicated that the energy transfer from HSA to diosmetin occurred with high possibility. The RLS and AFM results elucidated that diosmetin could interact with HSA and cause protein aggregation. The results of CD and FT−IR spectra indicated that the formation of HSA−diosmetin induced minimal conformational changes in the protein.

AUTHOR INFORMATION

Corresponding Author

*Tel: +8679188305234. Fax: +8679188304347. E-mail: gwzhang@ncu.edu.cn.

Funding

We gratefully acknowledge the financial support of the National Natural Science Foundation of China (Nos. 31060210 and 21167013), the Natural Science Foundation of Jiangxi Province (20114BAB204019), the Research Program of State Key Laboratory of Food Science and Technology of Nanchang University (SKLF-TS-200917 and SKLF-MB-201002) and the Foundation of Jiangxi Provincial Office of Education (GJJ11287).

Notes

The authors declare no competing financial interest.

REFERENCES

(1) Chi, Z. X.; Liu, R. T.; Teng, Y.; Fang, X. Y.; Gao, C. Z. Binding of oxytetracycline to bovine serum albumin: spectroscopic and molecular modeling investigations. *J. Agric. Food Chem.* **2010**, *58*, 10262−10269.

(2) Deng, F. Y.; Liu, Y. Study of the interaction between tosufloxacin tosylate and bovine serum albumin by multi-spectroscopic methods. *J. Lumin.* **2012**, *132*, 443−448.

(3) Zhang, G.. W.; Que, Q. M.; Pan, J. H.; Guo, J. B. Study of the interaction between icariin and human serum albumin by fluorescence spectroscopy. *J. Mol. Struct.* **2008**, *881*, 132−138.

(4) Subramanyam, R.; Gollapudi, A.; Bonigala, P.; Chinnaboina, M.; Amooru, D. G. Betulinic acid binding to human serum albumin: A study of protein conformation and binding affinity. *J. Photochem. Photobiol., B* **2009**, *94*, 8−12.

(5) Pan, X. R.; Qin, P. F.; Liu, R. T.; Wang, J. Characterizing the interaction between tartrazine and two serum albumins by a hybrid spectroscopic approach. *J. Agric. Food Chem.* **2011**, *59*, 6650−6656.

(6) Bani-Yaseen, A. D. Spectrofluorimetric study on the interaction between antimicrobial drug sulfamethazine and bovine serum albumin. *J. Lumin.* **2011**, *131*, 1042−1047.

(7) Dufour, C.; Dangles, O. Flavonoid−serum albumin complexation: determination of binding constants and binding sites by fluorescence spectroscopy. *Biochim. Biophys. Acta* **2005**, *1721* (1−3), 164−173.

(8) Zhang, J.; Wang, X. J.; Yan, Y. J.; Xiang, W. S. Comparative studies on the interaction of genistein, 8-chlorogenistein, and 3′, 8-dichlorogenistein with bovine serum albumin. *J. Agric. Food Chem.* **2011**, *59*, 7506−7513.

(9) Yang, Q.; Zhou, X. M.; Chen, X. G. Combined molecular docking and multi-spectroscopic investigation on the interaction between Eosin B and human serum albumin. *J. Lumin.* **2011**, *131*, 581−586.

(10) Vlasova, I. M.; Bukharova, E. M.; Kuleshova, A. A.; Saletsky, A. M. Spectroscopic investigations of interaction of fluorescent nanomarkers of fluorescein family with human serum albumin at different values of pH. *Curr. Appl. Phys.* **2011**, *11*, 1126−1132.

(11) Panovska, T. K.; Kulevanova, S; Stefova, M. In vitro antioxidant activity of some *Teucrium* species (Lamiaceae). *Acta Pharm.* **2005**, *55*, 207−214.

(12) Meirinhos, J.; Silva, B. M.; ValentÃo, P.; Seabra, R. M.; Pereira, J. A.; Dias, A.; Andrade, P. B.; Ferreres, F. Analysis and quantification of flavonoidic compounds from Portuguese olive (*Olea europaea* L.) leaf cultivars. *Nat. Prod. Res.* **2005**, *19*, 189−195.

(13) Mueller, M.; Hobiger, S.; Jungbauer, A. Anti-inflammatory activity extracts from fruits, herbs and spices. *Food Chem.* **2010**, *122*, 987−996.

(14) Morel, I.; Lescoat, G.; Cogrela, P.; Sergenta, O.; Pasdeloup, N.; Brissot, P.; Cillarda, P.; Cillarda, J. Antioxidant and iron-chelating activities of the flavonoids catechin, quercetin and diosmetin on iron-loaded rat hepatocyte cultures. *Biochem. Pharmacol.* **1993**, *45*, 13−19.

(15) Androutsopoulos, V. P.; Mahale, S.; Arroo, R. R. J.; Potter, G.. Anticancer effects of the flavonoid diosmetin on cell cycle progression and proliferation of MDA-MB 468 breast cancer cells due to CYP1 activation. *Oncol. Rep.* **2009**, *21*, 1525−1528.

(16) Maiti, T. K.; Ghosh, K. S.; Dasgupta, S. Interaction of (-)-epigallocatechin-3-gallate with human serum albumin: fluorescence, Fourier transform infrared, circular dichroism, and docking studies. *Proteins* **2006**, *64*, 355−362.

(17) Herskovits, T. T.; Gadegbeku, B.; Jaillet, H. On the structural stability and solvent denaturation of proteins. *J. Biol. Chem.* **1970**, *245*, 2588−2598.

(18) Li, Y.; Yao, X. J.; Jin, J.; Chen, X. G.; Hu, Z. D. Interaction of rhein with human serum albumin investigation by optical spectroscopic technique and modeling studies. *Biochim. Biophys. Acta* **2007**, *1774*, 51−58.

(19) Ahmad, B.; Parveen, S.; Khan, R. H. Effect of albumin conformation on the binding of ciprofloxacin to human serum albumin: a novel approach directly assigning binding site. *Biomacromolecules* **2006**, *4*, 1350−1356.

(20) Shi, X. L.; Li, X. W.; Gui, M. Y.; Zhou, H. Y.; Yang, R. J.; Zhang, H. Q.; Jin, Y. R. Studies on interaction between flavonoids and bovine serum albumin by spectral methods. *J. Lumin.* **2010**, *130*, 637−644.

(21) Lakowicz, J. R. *Principles of Fluorescence Spectroscopy*, 3rd ed.; Springer Publications: New York, 2006; p 282.

(22) Yuan, T.; Weljie, A. M.; Vogel, H. J. Tryptophan fluorescence quenching by methionine and selenomethionine residues of calmodulin: Orientation of peptide and protein binding. *Biochemistry.* **1998**, *37*, 3187−3195.

(23) Xu, J. G.; Wang, Z. B. *Methods of Fluorescence Analysis*, 3rd ed.; Science Press: Beijing, 2006; p 11.

(24) Lakowicz, J. R.; Weber, G. Quenching of fluorescence by oxygen: A probe for structural fluctuations in macromolecules. *Biochemistry* **1973**, *12*, 4161−4170.

(25) Wang, C.; Li, Y. Study on the binding of propiconazole to protein by molecular modeling and a multispectroscopic method. *J. Agric. Food Chem.* **2011**, *59*, 8507−8512.

(26) Lehrer, S. S. Solute perturbation of protein fluorescence. Quenching of the tryptophyl fluorescence of model compounds and of lysozyme by iodide ion. *Biochemistry* **1971**, *10*, 3254−3263.

(27) Ross, P. D.; Subramanian, S. Thermodynamics of protein association reaction: forces contributing to stability. *Biochemistry* **1981**, *20*, 3096−3102.

(28) Yuan, J. L.; Liu, H.; Kang, X.; Lv, Z.; Zou, G. L. Characteristics of the isomeric flavonoids apigenin and genistein binding to hemoglobin by spectroscopic methods. *J. Mol. Struct.* **2008**, *891*, 333−339.
(29) Yang, J.; Chen, X. D.; Fu, R. W.; Luo, W. A.; Li, Y. B.; Zhang, M. Q. Kinetics of phase separation in polymer blends revealed by resonance light scattering spectroscopy. *Phys. Chem. Chem. Phys.* **2010**, *12*, 2238−2245.
(30) He, Y. Q.; Liu, S. P.; Kong, L.; Liu, Z. F. A study on the sizes and concentrations of gold nanoparticles by spectra of absorption, resonance Rayleigh scattering and resonance non-linear scattering. *Spectrochim. Acta, A* **2005**, *61*, 2861−2866.
(31) Balashev, K.; Callisen, T. H.; Svendsen, A.; Bjørnholm, T. Savinase action on bovine serum albumin (BSA) monolayers demonstrated with measurements at the air−water interface and liquid Atomic Force Microscopy (AFM) imaging. *Colloids Surf., B.* **2011**, *88*, 582−586.
(32) Yang, Y.; Wang, H.; Erie, D. A. Quantitative characterization of biomolecular assemblies and interactions using atomic force microscopy. *Methods* **2003**, *29*, 175−187.
(33) Petitpas, I.; Grüne, T.; Bhattacharya, A. A.; Curry, S. Crystal structures of human serum albumin complexed with monounsaturated and polyunsaturated fatty acids. *J. Mol. Biol.* **2001**, *314*, 955−960.
(34) Privalow, P. L.; Gill, S. J. Stability of protein structure and hydrophobic interaction. *Adv. Protein Chem.* **1988**, *3*, 191−234.
(35) Sudlow, G.; Birkett, D. J.; Wade, D. N. Further characterization of specific drug binding sites on human serum albumin. *Mol. Pharmacol.* **1976**, *12*, 1052−1061.
(36) Sjoholm, I.; Ekman, B.; Kober, A.; Ljungstedt-Pahlman, I.; Seiving, B.; Sjodin, T. Binding of drugs to human serum albumin: XI. The specificity of three binding sites as studied with albumin immobilized in microparticles. *Mol. Pharmacol.* **1979**, *16*, 767−777.
(37) Maes, V.; Engelborghs, Y.; Hoebeke, J.; Maras, Y.; Vercruysse, A. Fluorimetric analysis of the binding of warfarin to human serum albumin. Equilibrium and kinetic study. *Mol. Pharmacol.* **1981**, *21*, 100−107.
(38) Dagher, R.; Pigault, C.; Bonnet, D.; Boeglin, D.; Pourbaix, C.; Kilhoffer, M. C.; Villa, P.; Wermuth, C. G.; Hibert, M.; Haiech, J. Use of a fluorescent polarization based high throughput assay to identify new Calmodulin ligands. *Biochim. Biophys. Acta* **2006**, *1763*, 1250−1255.
(39) Qi, Z. D.; Zhou, B.; Xiao, Q.; Shi, C.; Liu, Y.; Dai, J. Interaction of rofecoxib with human serum albumin: Determination of binding constants and the binding site by spectroscopic methods. *J. Photochem. Photobiol., A* **2008**, *193*, 81−88.
(40) Naik, P. N.; Chimatadar, S. A.; Nandibewoor, S. T. Interaction between a potent corticosteroid drug − Dexamethasone with bovine serum albumin and human serum albumin: A fluorescence quenching and fourier transformation infrared spectroscopy study. *J. Photochem. Photobiol., B* **2010**, *100*, 147−159.
(41) Carter, D. C.; Ho, J. X. Structure of serum albumin. *Adv. Protein Chem.* **1994**, *45*, 153−203.
(42) Förster, T.; Sinanoglu, O. *Modern Quantum Chemistry*, Academic Press: New York, 1966.
(43) Kanakis, C. D.; Tarantilis, P. A.; Polissiou, M. G.; Diamantoglou, S.; Tajmir-Riahi, H. A. Antioxidant flavonoids bind human serum albumin. *J. Mol. Struct.* **2006**, *798*, 69−74.
(44) Wu, F. Y.; Zhang, L. N.; Ji, Z. J.; Wan, X. F. Spectroscopic investigation of the interaction between thiourea-zinc complex and serum albumin. *J. Lumin.* **2010**, *130*, 1280−1284.
(45) Sarkar, D.; Mahata, A.; Das, P.; Girigoswami, A.; Ghosh, D.; Chattopadhyay, N. Deciphering the perturbation of serum albumins by a ketocyanine dye: A spectroscopic approach. *J. Photochem. Photobiol., B* **2009**, *96*, 136−143.
(46) Gao, W. H.; Li, N. N.; Chen, Y. W.; Xu, Y. P.; Lin, Y. J.; Yin, Y. G.; Hu, Z. D. Study of interaction between syringin and human serum albumin by multi-spectroscopic method and atomic force microscopy. *J. Mol. Struct.* **2010**, *983*, 133−140.
(47) Sandhya, B.; Hegde, A. H.; Kalanur, S. S.; Katrahalli, U.; Seetharamappa, J. Interaction of triprolidine hydrochloride with serumal bumins: Thermodynamic and binding characteristics, and influence of site probes. *J. Pharm. Biomed. Anal.* **2011**, *54*, 1180−1186.
(48) Khan, S. N.; Islam, B.; Yennamalli, R.; Sulta, A.; Subbarao, N.; Khan, A. U. Interaction of mitoxantrone with human serum albumin: Spectroscopic and molecular modeling studies. *Eur. J. Pharm. Sci.* **2008**, *35*, 371−382.
(49) Byler, D. M.; Brouilette, J. N.; Susi, H. Quantitative studies of protein structure by FT-IR spectra deconvolution and curve-fitting. *Spectroscopy* **1986**, *1*, 29−32.
(50) Liu, X. H.; Xi, P. X.; Chen, F. J.; Xu, Z. H.; Zeng, Z. Z. Spectroscopic studies on binding of 1-phenyl-3-(coumarin-6-yl)-sulfonylurea to bovine serum albumin. *J. Photochem. Photobiol., B* **2008**, *92*, 98−102.